

Optical, Redox, and DNA-Binding Properties of Phenanthridinium Chromophores: Elucidating the Role of the Phenyl Substituent for Fluorescence Enhancement of Ethidium in the Presence of DNA

Christa Prunkl,^[a] Markus Pichlmaier,^[b] Rainer Winter,^[b] Vladimir Kharlanov,^[c] Wolfgang Rettig,^{*,[c]} and Hans-Achim Wagenknecht^{*,[a]}

Abstract: The phenanthridinium chromophores 5-ethyl-6-phenylphenanthridinium (**1**), 5-ethyl-6-methylphenanthridinium (**2**), 3,8-diamino-5-ethyl-6-methylphenanthridinium (**3**), and 3,8-diamino-5-ethyl-6-(4-*N,N*-diethylaminophenyl)phenanthridinium (**4**) were characterized by their optical and redox properties. All dyes were applied in titration experiments with a random-sequence 17mer DNA duplex and their binding affinities were determined. The results were compared to well-known ethidium bromide (**E**). In general, this set of data allows the influence of substituents in positions 3, 6, and 8 on the optical properties of **E** to be elucidated. Especially, compound **4** was used to compare the weak electron-donating character of the phenyl substituent at position 6 of **E** with the more electron-donating 4-*N,N*-diethylaminophenyl

group. Analysis of all of the measurements revealed two pairs of chromophores. The first pair, consisting of **1** and **2**, lacks the amino groups in positions 3 and 8, and, as a result, these dyes exhibit clearly altered optical and electrochemical properties compared with **E**. In the presence of DNA, a significant fluorescence quenching was observed. Their binding affinity to DNA is reduced by nearly one order of magnitude. The electronic effect of the phenyl group in position 6 on this type of dye is rather small. The properties of the second set, **3** and **4**, are similar to **E** due to the presence of the two strongly electron-donating amino


groups in positions 3 and 8. However, in contrast to **1** and **2**, the electron-donating character of the substituent in position 6 of **3** and **4** is critical. The binding, as well as the fluorescence enhancement, is clearly related to the electron-donating effect of this substituent. Accordingly, compound **4** shows the strongest binding affinity and the strongest fluorescence enhancement. Quantum chemical calculations reveal a general mechanism related to the twisted intramolecular charge transfer (TICT) model. Accordingly, an increase of the twist angle between the phenyl ring in position 6 and the phenanthridinium core opens a nonradiative channel in the excited state that depends on the electron-donating character of the phenyl group. Access to this channel is hindered upon binding to DNA.

Keywords: charge transfer • DNA • dyes/pigments • fluorescent probes • intercalations

[a] Dipl.-Chem. C. Prunkl, Prof. Dr. H.-A. Wagenknecht
Institute for Organic Chemistry
University of Regensburg
Universitätsstraße 31
93053 Regensburg (Germany)
Fax: (+49) 941-943-4617
E-mail: achim.wagenknecht@chemie.uni-regensburg.de

[b] Dipl.-Chem. M. Pichlmaier, Prof. Dr. R. Winter
Institute for Inorganic Chemistry
University of Regensburg
Universitätsstraße 31
93053 Regensburg (Germany)

[c] Dr. V. Kharlanov, Prof. Dr. W. Rettig
Institute of Chemistry
Humboldt University Berlin
Brook-Taylor-Str. 3
12489 Berlin (Germany)
Fax: (+49) 30-2093-5574
E-mail: rettig@chemie.hu-berlin.de

 Supporting information for this article is available on the WWW under <http://dx.doi.org/10.1002/chem.200902823>.

Introduction

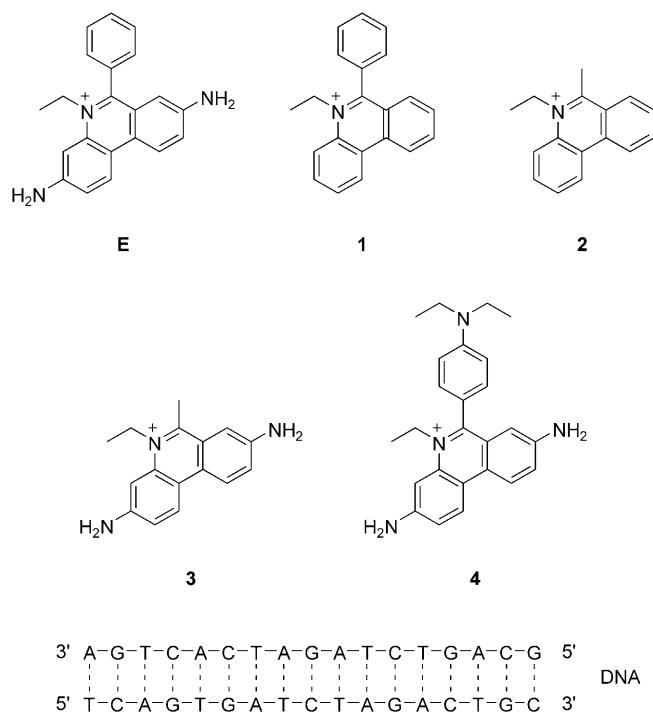
Planar polycyclic aromatic heterocycles ability to intercalate between two adjacent base pairs in duplex DNA was first proposed by Lerman.^[1] Among such intercalators, charged heterocycles are the most potent with respect to noncovalent stacking interactions. It is believed that the electrostatic energy plays an important role, not only for binding to nucleic acids, but also for the intercalation process.^[2,3] Accordingly, quinolizinium and acridizinium dyes have been developed as powerful fluorescent probes that light up upon intercalative binding to duplex DNA.^[4,5] 3,8-Diamino-5-ethyl-6-phenylphenanthridinium (Ethidium, **E**) represents the most prominent example of these positively charged heterocyclic intercalators for DNA (Scheme 1). It is widely used as a fluorescent staining agent for nucleic acids due to the significant emission increase upon binding to DNA or RNA, as intense research in the 1960's and 1970's revealed.^[6] The phenanthridinium compounds, including **E**, had their origin in the search for antitumor,^[7] as well as antiviral drugs,^[8] and most importantly for trypanocidal drugs.^[9,10] However, the application in human therapy is not reasonable due to the significant mutagenic and carcinogenic properties of **E**.^[11] Thus, research has been focused on the development of phenanthridinium intercalators for fluorescent DNA analytics. Mono- and bifunctional derivatives have been synthesized to modulate the binding properties of **E**.^[12] The photochemical reactivity of **E**^[13] has been applied to study photo-induced energy-transfer^[14] and charge-transfer (CT) processes in DNA.^[15–17] We developed a protocol for the synthetic

incorporation of the phenanthridinium heterocycle of **E** as an artificial DNA base through DNA building-block chemistry,^[18] and applied these conjugates in charge-transfer experiments^[17] and for the investigation of DNA–protein complexes.^[19]

Understanding the unique intercalation and emission properties of **E** has been the aim of a number of intense studies.^[10,20–24] This is of high importance for the development of new and improved fluorescent intercalators for molecular diagnostics with DNA and RNA. It has been proposed that enhancement of the emission of **E** is due to a proton transfer to the excited state of **E**, which is prevented upon intercalation into duplex DNA.^[20] It became clear that the amino groups in positions 3 and 8 of the phenanthridinium heterocycle of **E** are involved in this proton transfer. However, there are some serious doubts about this early proposal. Especially with respect to the current model of the intercalated structure of **E**, it is not clear why the two amino groups, which point out of the DNA duplex in the direction of the water layer, should be shielded from deprotonation. Early studies have shown that the exocyclic primary amino groups of **E** are not mandatory for the intercalation reaction, but that their presence adds stability to the complex with a nucleic acid.^[21] NMR spectroscopy studies by Leupin et al. using 3- and 8-deaminoethidium revealed that the removal of the 8-amino group had little effect on the binding to DNA, whereas the removal of the 3-amino group greatly affected the intercalation.^[25] The most recent study by Tor and co-workers showed the influence of such modifications on the electronic structure of **E**.^[26] This study included 5-ethyl-6-phenylphenanthridinium (3,8-dideaminoethidium, **1**) that was also previously described by others.^[24,27–29]

On the other hand, several theoretical chemical calculations have shown that the quaternization at position 5 adds significantly to the intercalation properties of phenanthridines.^[22–24] However, variation of the quaternizing group at position 5 has little or no effect on the intercalation properties.^[10,21] The stabilization energy of the cationic intercalators is considerably larger than those of the uncharged equivalents. The electron-poor phenanthridinium core stacks with the relatively electron-rich DNA bases and interaction is dominated by dispersion energy. The CT character seems to be important.^[22] Our studies with phenanthridinium incorporated as an artificial DNA base into oligonucleotides have also shown that the emission of this chromophore is slightly diminished in a G–C environment compared with a T–A environment, which might indicate a CT interaction, especially with the electron-rich guanines inside DNA.^[18]

According to the mentioned studies,^[10,22–24] it looked reasonable to synthesize phenanthridinium chromophores as derivatives of **E** to experimentally elucidate the role of the substituents with respect to the photophysical and DNA-binding properties, as well as the concomitant fluorescence enhancement. Early and basic steps in the synthesis of phenanthridinium derivatives were made by Walls and Morgan,^[30] Watkins et al.,^[27,31] and Berg.^[32] A variety of chemical modifications have been introduced synthetically



Scheme 1. Ethidium (**E**), the phenanthridinium chromophores **1–4**, and the DNA sequence that were used in this study.

to the amino functions at positions 3 and 8.^[24,26–29,33,34] Herein, we present the characterization of **1**, 5-ethyl-6-methylphenanthridinium (**2**), 3,8-diamino-5-ethyl-6-methylphenanthridinium (**3**), and 3,8-diamino-5-ethyl-6-(4-*N,N*-diethylaminophenyl)phenanthridinium (**4**) with respect to their optical and redox properties. Titration experiments with these intercalators and a 17mer DNA duplex (Scheme 1) allow the effects of the substituents in positions 3 and 8, but especially in position 6 of the core heterocycle on the DNA-binding properties to be elucidated. Phenanthridinium **3** is structurally similar to desphenyl dimidium, which was published by Waring and Wakelin.^[10] Derivative **4** was prepared to compare the weak electron-donating character of the phenyl substituent at position 6 of **E** with the stronger electron-donating 4-*N,N*-diethylaminophenyl group, which is similar to the published ethyl phenidium, but with the 3-amino group.^[10] Additionally, quantum chemical calculations were applied to investigate the effect of conformational relaxation on the efficiency of fluorescence enhancement upon intercalation into DNA. Accordingly, the difference in the fluorescence enhancement that was observed for **E** and **4** can be rationalized by a twisted intramolecular charge-transfer (TICT)-like model.

Results

Optical properties of chromophores 1–4: The phenanthridinium chromophores **1–4** were characterized by UV/Vis absorption and fluorescence spectroscopy and the spectra were compared with those of the commercially available and well-described **E**. With respect to the subsequent titration experiments with DNA, the optical characterization was performed in aqueous buffer solution (10 mM sodium phosphate, pH 7.0). The absorption spectra revealed two distinct classes of chromophores (Figure 1).

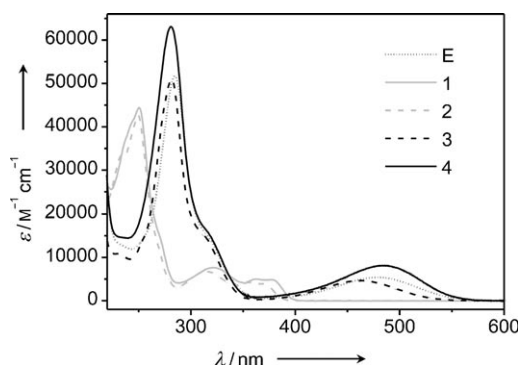


Figure 1. UV/Vis extinction spectra of the chromophores **1–4** in comparison with **E** ($c=23 \mu\text{M}$ in sodium phosphate buffer (10 mM, pH 7.0, $T=20^\circ\text{C}$)).

In comparison with **E**, the phenanthridinium dyes **1** and **2** exhibit altered absorption maxima at 251/322/377 nm (**1**) and 250/315/369 nm (**2**). It is noteworthy that our experi-

mentally determined extinction coefficients for chromophore **1** (Table 1) are in good agreement with the published values.^[34] In contrast, the phenanthridinium dyes **3** and **4**

Table 1. Characterization of the chromophores **E** and **1–4** by absorption and fluorescence spectroscopy and summary of the titration experiments with DNA; sodium phosphate buffer (10 mM, pH 7.0, $T=20^\circ\text{C}$) was used for all measurements.

	Absorption				Fluorescence			
	Without DNA	With DNA ^[a]	Without DNA	With DNA ^[a]	Without DNA	With DNA ^[a]	Without DNA	With DNA ^[a]
	λ_{max} [nm]	ϵ [$\text{M}^{-1}\text{cm}^{-1}$]	λ_{max} [nm]	$\Delta\lambda_{\text{max}}$ [nm]	λ_{max} [nm]	Φ_F	λ_{max} [nm]	$\Delta\lambda_{\text{max}}$ [nm]
E ^[c]	285	51 950	— ^[b]	—	615	0.01 ^[e]	601	14
	479	5420	522	43				
1 ^[d]	251	44 250	— ^[b]	—	420	0.24 ^[f]	420	0
	322	7640	325	3				
	377	4880	378	1				
2	250	42 460	— ^[b]	—	407	0.35 ^[f]	407	0
	315	6640	320	5				
	369	3830	369	0				
3 ^[g]	282	50830	— ^[b]	—	599	0.02 ^[e]	583	16
	463	4640	503	40				
4 ^[h]	281	63 310	— ^[b]	—	616	(0.0001) ^[i]	601	15
	486	8180	528	42				

[a] 213.6 μM DNA-bp for absorption, 109.3 μM DNA-bp for fluorescence. [b] Not determined due to DNA absorption. [c] Published values:^[33] 285 (56800), 478 (5680); and 480 nm ($6300 \text{ M}^{-1}\text{cm}^{-1}$).^[10] [d] Published values:^[29] 251 (43040), 321 (7700), 377 nm ($4770 \text{ M}^{-1}\text{cm}^{-1}$). [e] Fluorescence quantum yield determined with rhodamine 101 as a reference^[36] ($\Phi_F=1.0$). [f] Fluorescence quantum yield determined with quinine sulfate as a reference^[36] ($\Phi_F=0.546$). [g] Compared with published values for desphenyl dimidium:^[10] 470 nm ($4220 \text{ M}^{-1}\text{cm}^{-1}$). [h] Compared with published values for ethyl phenidium:^[10] 430 nm ($5380 \text{ M}^{-1}\text{cm}^{-1}$). [i] Fluorescence quantum yield determined relative to **E**, but given relative to rhodamine 101.

showed absorption maxima at 282/463 nm (**3**) and 281/486 nm (**4**) that are similar to **E** (285/479 nm). Moreover, chromophores **3** and **4** display absorption bands in the range 460–490 nm due to the CT character, similar to **E**. The extinction coefficient for chromophore **3** at 463 nm ($4640 \text{ M}^{-1}\text{cm}^{-1}$) is clearly lower than the corresponding value of chromophore **4** at 486 nm ($8180 \text{ M}^{-1}\text{cm}^{-1}$) and **E** at 479 nm ($5420 \text{ M}^{-1}\text{cm}^{-1}$).

The steady-state fluorescence spectra also reveal two different classes of chromophores. Dyes **1** and **2** exhibit emission spectra with maxima at 420 and 407 nm, respectively (Figure 2). For both compounds, Stokes shifts of about 40 nm are observed. In contrast, the fluorescence of chromophores **3** and **4** show larger bathochromic shifts (in the range of 130 nm), which are characteristic for **E**. The emission maxima were observed at 599 nm (**3**), and 616 nm (**4**).

Due to the optical differences between chromophores **1** and **2**, and dyes **E**, **3**, and **4**, different standards for the determination of fluorescence quantum yields had to be used (see the Supporting Information).^[35,36] Chromophores **1** and **2** are both highly fluorescent in aqueous buffer solution, with quantum yields of 0.24 (**1**) and 0.35 (**2**). Compounds **3** and **4** exhibit strong fluorescence quenching; the quantum yields are 0.01 (**E**) and 0.02 (**3**). The fluorescence quantum

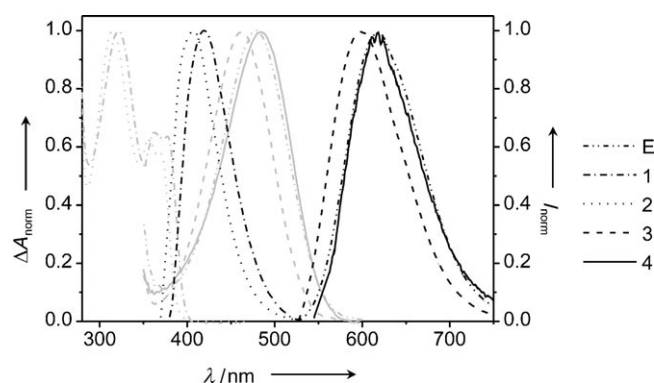


Figure 2. Normalized UV/Vis absorption (gray lines) and fluorescence (black lines) spectra of chromophores **1–4** in comparison with **E**. Dashed lines: normalized absorption ($c=23\ \mu\text{M}$); solid lines: normalized fluorescence ($c=2.4\ \mu\text{M}$), in sodium phosphate buffer (10 mM, pH 7.0, $T=20\ ^\circ\text{C}$).

yield of **4** was too low to be determined with rhodamine 101 as the reference. To obtain a rough estimation, the quantum yield was determined relative to **E** and calculated to be about 100 times lower in aqueous buffer solution.

Redox characterization: To characterize chromophores **1–4** electrochemically, we measured the reduction potential by cyclic voltammetry. It is important to note that the reduction potentials of compounds **2** and **3** were obtained irreversibly. Chromophores **1** and **2** show reduction potentials of -1.34 and -1.36 V, respectively (Table 2). When compared with **E** (-1.53 V), these potentials reflect the absence of the elec-

Table 2. Electrochemical characterization of **E** and **1–4**.

Reduction	$E_{1/2}$ [V] ^[a]	E_{00} [eV]	E^* [eV] ^[b]
E ⁺ / E [•]	-1.53	2.2	0.7
1 ⁺ / 1 [•]	-1.34	3.2	1.8
2 ⁺ / 2 [•]	-1.36 ^[c]	3.2	1.9
3 ⁺ / 3 [•]	-1.67 ^[c]	2.3	0.6
4 ⁺ / 4 [•]	-1.62	2.2	0.6

[a] Measured by cyclic voltammetry in MeCN (50 mM NBu_4PF_6 as the supporting electrolyte) versus Fc^+/Fc as internal standard ($v=200\ \text{mVs}^{-1}$). [b] Excited-state potentials, calculated according to $E^*(\text{X}^+/\text{X})=E_{00}+E_{1/2}(\text{X}^+/\text{X})$.^[37] [c] Irreversible potentials.

tron-donating amino substituents, making **1** and **2** more readily reducible at less negative potentials. By using an E_{00} value of 3.2 eV for both chromophores, the reduction potentials of the excited state can be estimated as 1.8 eV (**1**) and 1.9 eV (**2**).^[37] Hence, both chromophores exhibit excited-state redox potentials that are significantly larger than that of **E**.

In contrast, the phenanthridinium chromophores **3** and **4** showed reduction potentials of -1.67 and -1.62 V, respectively, which are more negative than the corresponding value for **E**. When the E_{00} values of 2.3 eV (**3**) and 2.2 eV (**4**) were included in the calculation, the excited-state poten-

tials of both chromophores were calculated to be approximately 0.6 eV. This value is slightly lower than that of **E** (0.7 eV), which means that the dyes **3** and **4** are less easily reduced than **E**.

Titration experiments of chromophores 1–4 with DNA: To compare changes in the optical properties of chromophores **1–4** with **E** upon binding to DNA, we performed titration experiments with a representative synthetic 17mer DNA duplex with a random sequence (Scheme 1). To avoid dilution of the analyte solutions, the titrant solutions contained DNA (for absorption: $357\ \mu\text{M}$ DNA-bp, for fluorescence: $192\ \mu\text{M}$ DNA-bp) as well as the corresponding chromophore (for absorption: $23\ \mu\text{M}$, for fluorescence: $2.4\ \mu\text{M}$) in the same concentration as in the titrated solution. Aliquots (500 μL) of the chromophore solutions in Na-P_i-buffer were titrated in 5, 10, 20, 50, and 100 μL steps. Measurements exclude the region of the DNA absorption below 300 nm. Since the interaction with DNA also leads to significant changes in the absorption spectra of the chromophores, the excitation wavelengths for the fluorescence titrations were set to the corresponding isosbestic points, which were determined for each chromophore by spectrophotometric titrations.

The following titration with **E** serves as a reference: The UV/Vis spectrum of **E**, in the absence of DNA, showed an absorption with a maximum at 479 nm, which is typical for “free” **E** in water (Figure S1 in the Supporting Information).^[38] With increasing amounts of DNA, the maximum shifts to 522 nm, which is characteristic for intercalated **E**.^[22,39] The isosbestic point at 510 nm shows the transition between the unbound and the DNA-bound form of the dye. Upon excitation at 510 nm, the corresponding fluorescence of **E** in water (Figure S3 in the Supporting Information) is weak and has a maximum at 615 nm. With increasing DNA concentration, the emission increases significantly and the maximum shifts to 601 nm.

Subsequent titrations with **1–4** show two pairs of chromophores, as already pointed out in the previous sections with respect to the optical and the redox properties. The absorption spectra of **1** (maxima at 322, 364 and 377 nm; Figure 3) and **2** (maxima at 315, 356 and 369 nm; Figure S2 in the Supporting Information) show a decrease in the extinction with DNA, accompanied by a rather small shift (3–5 nm) and a broadening of the signals. When excited at 388 (**1**) or 378 nm (**2**), the fluorescence maxima can be observed at 420 or 407 nm, respectively. The fluorescence of both chromophores is quenched significantly in the presence of DNA (**1**: Figure 4, **2**: Figure S4 in the Supporting Information), but the quenching is not accompanied by a shift of the corresponding maxima.

In contrast to **1** and **2**, chromophores **3** and **4** exhibit an **E**-like behavior in the titration experiments with DNA. The absorption maximum of phenanthridinium **3** shifts from 463 nm in the unbound form to 503 nm in the bound form (Figure 3); the absorption maximum of **4** shifts from 486 to 528 nm (Figure S2 in the Supporting Information). The isosbestic points at 492 or 510 nm, respectively, support the

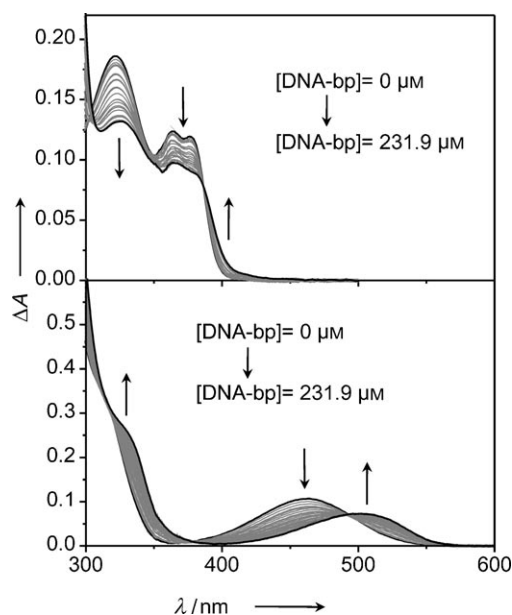


Figure 3. Representative titration experiments of chromophores **1** and **3** with DNA followed by UV/Vis absorption spectroscopy. Upper graph: spectrophotometric titration of double-stranded (ds)-DNA to **1** ($c = 23 \mu\text{M}$) in sodium phosphate buffer (10 mM, pH 7.0, $T = 20^\circ\text{C}$); lower graph: spectrophotometric titration of ds-DNA to **3** ($c = 23 \mu\text{M}$) in sodium phosphate buffer (10 mM, pH 7.0, $T = 20^\circ\text{C}$). Arrows indicate changes in the intensity of the bands upon increasing DNA concentrations.

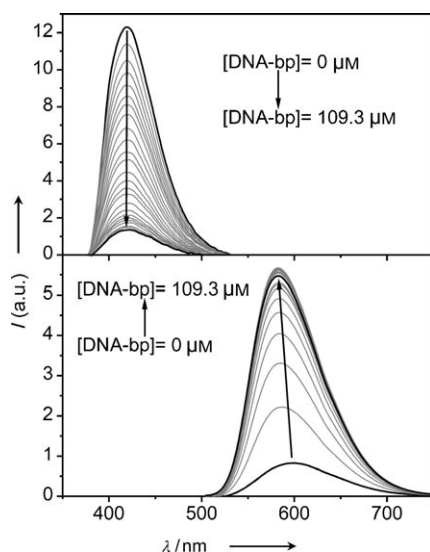


Figure 4. Representative titration experiments of chromophores **1** and **3** with DNA followed by fluorescence spectroscopy. Upper graph: fluorimetric titration of ds-DNA against **1** ($c = 2.4 \mu\text{M}$) in sodium phosphate buffer (10 mM, pH 7.0, $T = 20^\circ\text{C}$); lower graph: fluorimetric titration of ds-DNA against **3** ($c = 2.4 \mu\text{M}$) in sodium phosphate buffer (10 mM, pH 7.0, $T = 20^\circ\text{C}$). Arrows indicate changes in the intensity of the band upon increasing DNA concentrations.

idea of a single transition from unbound molecules to DNA-bound species.

The fluorescence spectra of the phenanthridiniums **3** and **4**, in the presence of DNA, also show E-like profiles. In

both cases, the emission intensity increases significantly when the chromophores are excited at 492 (**3**; Figure 4) or 510 nm (**4**; Figure S4 in the Supporting Information). This fluorescence enhancement is accompanied by a shift of the corresponding maximum, in the case of **3** from 599 nm without DNA to 583 nm with DNA, in the case of **4** from 616 to 601 nm.

In addition, an analysis of the spectrophotometric titrations according to McGhee and von Hippel^[40] (Figure S5 in the Supporting Information) was used to determine the association constants (K) between the chromophores **1–4** and DNA, as well as the binding-site sizes (n ; Table 3). For the

Table 3. Binding constants and binding-site sizes of the chromophores **E** and **1–4** as determined from spectrophotometric titrations with DNA in sodium phosphate buffer (10 mM, pH 7.0, $T = 20^\circ\text{C}$).

Compound	$K \times 10^5 \text{ [M}^{-1}\text{]}^{[a]}$	$n^{[b]}$
E	$5.0 \pm 0.3^{[c,d]}$	$1.6 \pm 0.1^{[c]}$
1	$0.46 \pm 0.05^{[d]}$	2.8 ± 0.2
2	0.67 ± 0.05	2.7 ± 0.1
3	$3.1 \pm 0.4^{[e]}$	$1.5 \pm 0.1^{[e]}$
4	$7.8 \pm 1.6^{[f]}$	$1.9 \pm 0.1^{[f]}$

[a] K is the binding constant (in bp). [b] n is the binding-site size (in bp). [c] Compared with published values for **E** at higher salt concentration (1 M NaCl):^[10] $K = 1.99 \times 10^4 \text{ M}^{-1}$, $n = 1.90$. [d] Similar to published values.^[43] [e] Compared with published values for desphenyl dimidium at higher salt concentration (1 M NaCl):^[10] $K = 1.13 \times 10^4 \text{ M}^{-1}$, $n = 1.73$. [f] Compared with published values for ethyl phenidium at higher salt concentration (1 M NaCl):^[10] $K = 9.63 \times 10^3 \text{ M}^{-1}$, $n = 1.87$.

titration of reference compound **E** with DNA, a binding constant of $5.0 \times 10^5 \text{ M}^{-1}$ and a binding-site size of 1.6 (in bp) was observed. Both values are in good agreement with the results published by Zimmermann and Pauluhn^[41] and Horowitz and Hud,^[42] but are higher than the values reported by Waring and Wakelin,^[10] probably due to a lower salt concentration in our experiments. The binding constants for chromophores **1–4** again indicate two groups of chromophores. For chromophores **3** and **4**, the binding constants are in the 10^5 M^{-1} range ($3.1 \times 10^5 \text{ M}^{-1}$ for **3**, $7.8 \times 10^5 \text{ M}^{-1}$ for **4**). Remarkably, chromophore **4** exhibits a stronger binding to DNA than the reference **E**. The values found for chromophores **1** and **2** (5×10^4 and $7 \times 10^4 \text{ M}^{-1}$), however, are about one order of magnitude lower than that of **E**. Binding-site sizes were found to be in the range of 1.5–2.8 (in bp) for all chromophores, which is consistent with an intercalative binding mode according to the neighbor exclusion model.

Discussion

The optical, redox, and DNA-binding properties of the phenanthridinium dyes **1–4** reveal the electron-donating effects of the substituents in positions 3, 8, and especially 6, on the electron-poor phenanthridinium core system. It became evident from our optical and electrochemical characterization, as well as from the titration experiments with DNA, that

the dyes can be divided into two pairs. The first pair (**1** and **2**) lacks the two exocyclic amino groups in positions 3 and 8, chromophore **2** additionally lacks the phenyl group in position 6. Compared with **E**, both chromophores have significantly altered optical, electrochemical, and DNA-binding properties. As a result of the lack of CT contribution by the amino groups, both the absorption and the emission of **1** and **2** occur at shorter wavelengths. The emission intensities in aqueous buffer solutions are higher ($\Phi_F=0.24$ for **1** and $\Phi_F=0.35$ for **2**) compared with **E** ($\Phi_F=0.01$) and the Stokes' shifts are small (ca. 40 nm). It is important to point out that the minor difference of the optical properties between both chromophores can be attributed to the rather weak electron-donating character of the phenyl group in position 6 of **1**, which is absent in **2**. The observation that these differences between **1** and **2** are rather small indicates that electron donation by the phenyl group in position 6 is significantly weaker than the two exocyclic amines in positions 3 and 8.

In the DNA titration experiments with dyes **1** and **2**, a strong fluorescence quenching was observed that was nearly identical for both chromophores (Figure 5, top). The electrochemical potentials of both chromophores give a possible explanation for this observation. As mentioned in the previous section, the excited-state potentials can be estimated to have values of approximately 1.8 (**1**) and 1.9 eV (**2**). The potential for the oxidation of guanine (G^+/G) is 1.3 V versus NHE.^[43] By using a correction value of -0.63 V from the NHE to Fc/Fc^+ (Fc =ferrocene) reference,^[44] the corresponding guanine potential is approximately 0.7 V versus Fc/Fc^+ . This means that both phenanthridinium dyes, **1** and **2**, are potentially able to photooxidize guanines in the DNA. Such photoinduced processes between organic dyes

and the bases are often observed^[45] and have been widely used to study CT in DNA.^[46]

In contrast to the first pair, the second pair of chromophores (**3** and **4**) exhibits similarities with **E** due to the presence of the two amino groups in positions 3 and 8, yielding more electron-rich compounds. It is important to emphasize that the observed differences between **3**, **4**, and **E** can be assigned solely to the different substituents at position 6. Dye **3** lacks the weak electron-donating phenyl group completely, whereas dye **4** has the significantly stronger electron-donating 4-*N,N*-diethylaminophenyl group. The increasing electron-donating character of the substituents in position 6 orders the chromophores by their optical properties. The absorption maxima shifts from 463 (**3**) through 479 (**E**) to 486 nm (**4**), the emission maxima shifts from 599 (**3**), through 615 (**E**) to 616 nm (**4**), and the fluorescence quantum yield decreases from 0.02 for **3** to 0.01 for **E**; the fluorescence intensity of chromophore **4** is about 100 times lower than for **E** (in fact, Φ_F of **4** was too low to be determined by standard methods). Clearly, the CT contribution in these dyes increases with the electron-donating character of the substituent in position 6. This will be further discussed based on quantum chemical calculations in the next section.

In contrast to the optical properties, the redox potentials of chromophores **3** and **4** do not follow such a clear trend. Both potentials (-1.67 V for **3**; -1.62 V for **4**) were more negative than that of **E**. It is generally assumed that the photoexcited state of **E** cannot oxidize guanines^[47] and, based on the calculated excited-state potential of 0.6 eV as mentioned in the previous section, neither compound **3** nor **4** should be able to photooxidize guanines in DNA.

Luedtke et al. recently reported that the aromatic nitrogen and some carbon atoms of **E** have surprisingly high electron densities.^[26] This means that electron donation by the two exocyclic amines of **E** has a significantly larger effect compared to the electron-withdrawing influence of the endocyclic iminium core. The results of our experimental study on the substituent effects in chromophores **1–4** presented herein, strongly support this interpretation. Compared to chromophores **1** and **2**, the most notable differences between the chromophores **3**, **E**, and **4**, are the significant bathochromic shift of the absorption spectra and the remarkable increase in the fluorescence intensity that is observed during the titration experiments with DNA (Figure 5, bottom). When excited at the corresponding isosbestic point, as revealed by the spectrophotometric titrations, the dye **3** exhibits an approximately 7-fold increase in fluorescence intensity, which is lower than the 10-fold increase observed with **E**; in contrast, dye **4** shows a 21-fold increase. There is clearly a relationship between the substituent in position 6 of the phenanthridinium core and both the quantum yield in buffer (without DNA) and the fluorescence enhancement upon addition of duplex DNA. With increasing electron-donating character of the substituent in position 6, the fluorescence enhancement is more strongly pronounced in the presence of DNA, whereas the basic fluorescence without DNA is quenched more strongly. This can

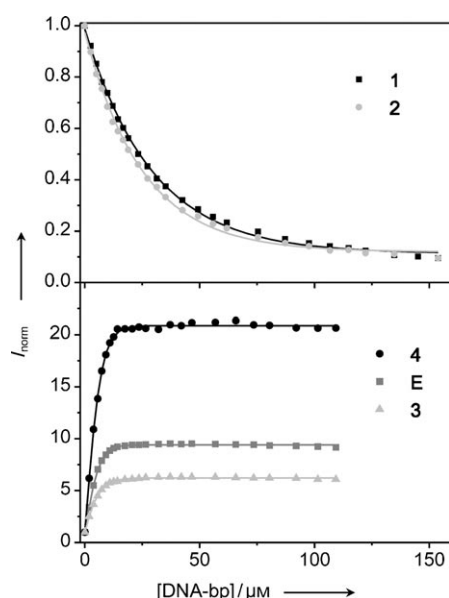


Figure 5. Titration curves for the spectrofluorimetric titrations of ds-DNA to **E** and chromophores **1–4**; $c=2.4$ μ M in sodium phosphate buffer (10 mM, pH 7.0, $T=20$ °C).

be explained by a TICT-like model as described in the next section. According to this model, the nonradiative channel in the excited-state, which leads to the small fluorescence quantum yield in solution without DNA, is more pronounced with a stronger electron-donating substituent in position 6. Access to this channel involves a twist of the phenyl ring against the plane of the phenanthridinium core. The necessary angular relaxation occurs in solution without DNA, but is hindered by intercalation in the presence of DNA, leading to the fluorescence enhancement.

Additionally, the binding constants that were determined for chromophores **1–4** with DNA reflect the strong influence of the electron-donating exocyclic amino groups. Similar to **E**, the binding constants of **3** and **4** are in the 10^5 M^{-1} range ($3.1\text{--}7.8 \times 10^5 \text{ M}^{-1}$), whereas the values for **1** and **2** are reduced by nearly one order of magnitude ($5\text{--}7 \times 10^4 \text{ M}^{-1}$). Moreover, parallel to the reduction of the binding affinity of **1** and **2**, the binding-site sizes are significantly enhanced (2.7–2.8 base pairs) compared with those of **E**, **3**, and **4** (1.5–1.9 base pairs). The binding constants for **E**, **3**, and **4** are in a similar range to those observed for phenanthridinium–nucleotide conjugates ($\log K = 5.5\text{--}6.0$).^[48] Furthermore, the binding affinity of chromophores **3**, **E**, and **4** increases concomitantly with the enhanced electron-donating character of the phenyl substituent in position 6. Accordingly, dye **4** shows the strongest binding affinity. Hence, the binding affinity, as well as the fluorescence enhancement, is clearly related to the overall supply of electron density in the phenanthridinium heterocycle by the corresponding electron-donating substituents, not only in positions 3 and 8. It is remarkable that, according to our studies, the electron-donating character of the phenyl ring in position 6 of the phenanthridinium core is also crucial, especially in the presence of DNA. This observation is supported by quantum chemical calculations.

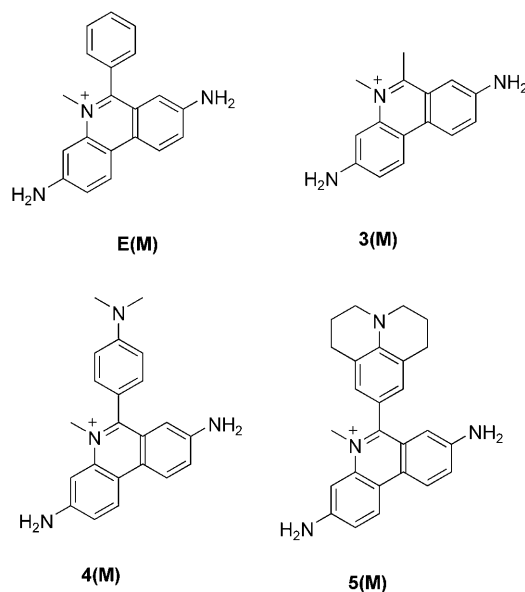
Quantum chemical calculations: The results showing fluorescence enhancement upon intercalation with DNA in Figure 5 indicate that the efficiency increases in the order **3** < **E** < **4**. It is possible that for **E** a conformational relaxation of the phenyl plays some role for this efficiency. This led us to look for a generally applicable mechanism whereby conformational relaxations of the substituted phenyl groups play a decisive role in the fate of the excited state.

A long-standing observation is the vastly different fluorescence quantum yield of rhodamine dyes (very large quantum yield) and their counterparts in which the bridge between the dialkylanilino groups is missing, such as in malachite green (MG) or crystal violet (CV) derivatives (extremely small quantum yield in fluid solvents). In the latter group, the quantum yield is strongly enhanced if the twisting relaxation is hindered by the medium (e.g., in highly viscous solutions).^[49,50] Clearly, the possibility of twisting an anilino group in these compounds creates a strong nonradiative channel. It has been proposed that the mechanism of this nonradiative channel is connected to a CT process,^[50–52] that is, the channel is only introduced if the group that can be

twisted is a sufficiently good electron donor. This has been highlighted in a rhodamine derivative with a flexible dialkylanilino group, with the expected fluorescence quenching occurring with high efficiency. If the dialkylanilino group is protonated and transformed into a weak acceptor, the quenching channel is blocked, and the quantum yield increases by a factor of 290.^[53]

This mechanism is closely related to the TICT theory of excited states in which CT and twisting are combined and the maximum CT is observed for the perpendicular conformation. In some cases, dual fluorescence can arise, whereas, in other cases, only the fluorescence quenching of the precursor state is observed; this could be induced by the relaxation of the pending donor group towards the perpendicular conformation.^[51,52] Applying this mechanism to the group of phenanthridinium compounds investigated herein, we can predict that if the phenyl group in **E** is exchanged for a better donor, such as a dialkylanilino (D) group, a low-lying excited CT state may also come into energetic reach and, possibly, enhance the fluorescence quenching observed for **E** in fluid solutions. Just as in the case of the di- or triphenylmethane dyes (e.g., MG and CV), inhibition of the twisting relaxation of the D group slows down the nonradiative channel. A simple explanation for the very strong fluorescence enhancement observed for **4** in DNA is therefore that this CT mechanism is partially involved, and that the relaxation is (partially or completely) blocked in the DNA environment.

To test this hypothesis, we performed quantum chemical calculations on model structures of **E**, **3**, and **4**, as well as on an additional derivative **5** (Scheme 2), which is predicted from the model to show a stronger enhancement of this CT quenching mechanism. In the first step, we used semiempirical AM1/ZINDO calculations to compare the four com-



Scheme 2. Structures of the model compounds used for the quantum chemical calculations.

pounds. In the second step, the high-level *ab initio* method DFT was used to confirm these results. These demanding calculations could only be performed for one compound; in this work we chose to investigate compound **4**.

Table 4 shows that our calculations for the ground-state equilibrium geometry indicate a good agreement between the calculated transition energy and the experimental results

Table 4. Comparison of experimental and calculated spectral characteristics of some ethidium derivatives.^[a]

Experimental structure	E	3	4	–
Calculated model structure	E(M)	3(M)	4(M)	5(M)
exp. fluorescence enhancement	10	7	21	nd
ΔE_{01} (exp.) [eV]	2.6	2.7	2.6	nd
ΔE_{01} (eq, calcd) [eV]	2.61	2.55	2.53	2.46
extinction coefficient [$M^{-1} cm^{-1}$]	5420	4640	8180	nd
oscillator strength f (calcd)	0.29	0.24	0.42	0.41
equilibrium twist angle ϕ (eq, calcd) [°]	84	–	67	64
S_0 barrier to 90° [cm^{-1}]	22	–	32	137
ΔE_{01} (90°, calcd) [eV]	2.59	–	2.65 ^[b]	2.52 ^[c]
ΔE_{CT-LE} (90°, calcd) [eV] ^[d]	0.95	–	0.01	–0.12

[a] Ground-state geometry optimizations were performed by applying the AM1 method. Excited-state characteristics (transition energies ΔE_{01} and energy differences derived thereby, as well as oscillator strengths, f) were calculated by using ZINDO/s for the AM1-optimized ground-state structure. Determination of the nature of the excited states involved an analysis of the orbitals and the configuration interaction matrix. [b] S_1 (LE) and S_2 (CT) are nearly degenerate. [c] S_1 (CT), S_2 (LE). [d] Energy difference from S_1 (CT) to the next higher (LE) state. nd: not determined.

for the absorption band maximum; the calculations also allow the localized nature of the lowest lying excited-state S_1 to be confirmed. The calculated oscillator strength increases in the same order as the experimental extinction coefficients (**3(M)** < **E(M)** < **4(M)**).

If the 90° twisted conformation is considered, either full CT from the D group to the phenanthridinium group (P) is possible, or the electron of the donor does not leave D, and the distribution of the positive charge rests as it is (localized on P). In this case, the corresponding excited state is termed locally excited (LE). When the LE and CT states are compared, the positive charge is localized on different parts of the molecule; hence, the CT process leading from LE to CT is connected with a change of localization of the positive charge on the donor D, corresponding to a charge shift towards D. If an excited CT state is within energetic reach on the S_1 hypersurface, it can be populated from the initially reached equilibrium LE state in which the positive charge is largely localized on the P moiety and leads to fluorescence quenching as discussed below.

The large charge shift in the CT state also causes an energy lowering in polar solvents. This can be explained in the following way: Any distribution of charges in a positively charged system, such as **4**, can be developed into a multipole expansion,^[54] in the simplest case, comprising a monopole and a dipole. The dipolar component leads to an additional energetic stabilization by polar solvents. We can therefore expect that the gas-phase energy values calculated

herein for the CT state are significantly lower in polar solvents due to the solvent interaction with the positive charge. This lowering is larger for the CT than for the LE state due to the additional dipolar contribution for the CT state. The consequence is that the CT state becomes energetically more easily accessible from the LE state and, as a result, an increase of the fluorescence quenching with increase of solvent polarity is expected. Experimentally, this has been studied in detail for a derivative of **4**, in which the P moiety is exchanged for a pyridinium group.^[55] The quantum chemical results obtained for this molecule are similar to those of **4**, that is, a CT state with full charge localization can be reached by angular relaxation to 90° twist.^[56]

The results of the DFT calculations (Figures 6 and 7) for **4(M)** confirm the full CT nature of the excited state at the orthogonal geometry, with full localization of the positive

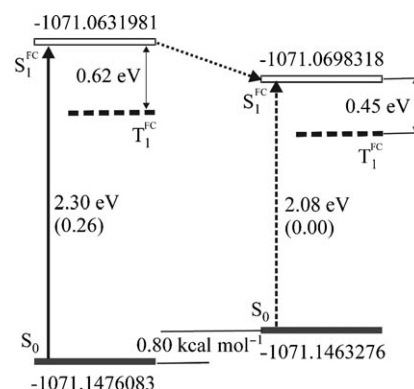


Figure 6. Qualitative scheme of the ground (S_0) and excited states (S_1^{FC} and T_1^{FC}) for **4(M)**. The energies of the states are calculated by B3LYP (ground states) and TDB3LYP (excited states), with basis set 6-31+G-(2df,2p) for the optimized equilibrium (left) and orthogonal (right) structures of **4(M)**. Absolute energies are given in Hartree units, energy differences in eV. Values in parenthesis are calculated oscillator strengths.

charge on the donor moiety, consistent with the TICT model. Such a CT state is connected with 1) a strong charge shift; 2) a vanishing transition moment, causing a very small oscillator strength as well as emissive rate constant; 3) a large nonradiative rate constant, causing strong fluorescence quenching; 4) a very close-lying CT triplet state that can also cause fast depopulation of the excited singlet state. The three factors 2), 3), and 4) reduce the fluorescence quantum yield by intrinsic photophysical processes of the twisted CT state, factor 1) leads to an energetic lowering of CT in polar solvents, resulting in a larger population of this state. The control parameters for the fluorescence quenching (or enhancement) are the polarity of the medium and the possibility of the twist relaxation, which is influenced by the rigidity of the surroundings.

Figure 6 shows that the relaxation from LE to CT is energetically favorable, and that the energy gap to the ground state and the first triplet state is reduced, causing enhanced nonradiative deactivation for CT. Moreover, as expected by the TICT model, a higher lying triplet state of CT nature is

isoenergetic with the CT singlet state at 90°. In contrast to CT, the positive charge remains on the phenanthridinium fragment ($\pi\pi^*$ state) for a pure LE state. For the equilibrium geometry (S_1^{FC} state), some charge is transferred to D due to weak CT π interactions, but the main character is LE. This can be seen in the frontier molecular orbitals for this geometry, which are somewhat delocalized (Figure 7). For the 90° geometry, however, the orbitals involved in the excitation (Figure 7) are localized on the P and D moieties and confirm the full CT nature, which causes the vanishing oscillator strength and large charge shift.

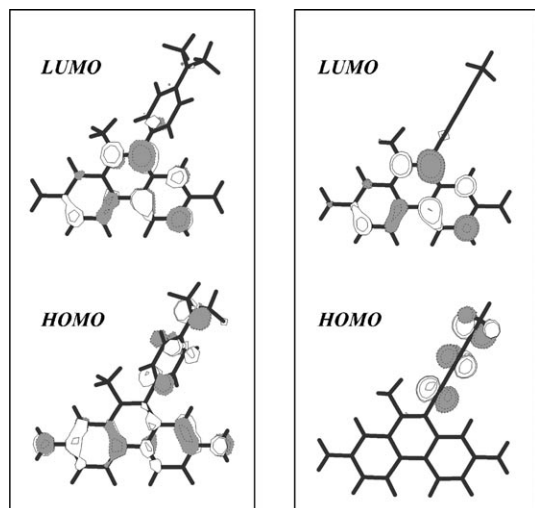


Figure 7. The HOMO and LUMO orbitals determining the main electronic configuration of the S_1^{FC} excited state for the optimized equilibrium (62.6° twist, left panel) and orthogonal (right panel) geometries of the cation **4(M)**. For the orthogonal geometry, a full electron leaves the donor moiety D towards P upon HOMO–LUMO excitation (CT state), and the positive charge is transferred in the opposite direction towards D. For the equilibrium geometry, this charge shift is reduced due to orbital delocalization (left panel).

Comparison of the four compounds listed in Table 4, using the AM1 and ZINDO methods, indicate that this combined method overestimates the energy of the CT state with respect to that of the LE state, compared with the DFT method, however, the energetic distance is still small enough for thermal population.

In **5(M)**, the CT state is expected to be further lowered in energy with respect to the LE state due to the better donor character of the julolidino group than the dimethylanilino group in **4(M)**; the calculations confirm these expectations. CT is the lowest excited state at 90°, with a gap of 0.12 eV to the next (LE) state. For **E(M)**, with the phenyl group as a very weak donor, the CT energy is very high and this mechanism plays a reduced role. In solution, the LE–CT energy gap will be somewhat modified with respect to our gas-phase calculations by the influence of the polar solvent.

In summary, five possible factors controlling the fluorescence enhancement on the basis of a TICT state can be discussed: The population of CT is controlled by 1) the rigidity

of the medium, allowing the twisting relaxation, and 2) by the energetic availability of the CT state, which is controlled by the donor strength and the medium polarity. The fluorescence quantum yield reduction in the CT state can occur by 1) the intrinsically very small radiative rate constant of this state; 2) by an enhancement of the nonradiative rate constant generally observed for TICT states and explainable by the reduction of the S_1 – S_0 energy gap, and 3) by a triplet state that is energetically similar. On the basis of the calculations summarized in Table 4, we can predict that a compound related to **5(M)** could give rise to an experimental fluorescence enhancement even larger than that of **4**.

Conclusion

To elucidate experimentally the role of the substituents in positions 3, 8, and especially 6 of the core heterocycle of **E** with respect to the photophysical and DNA-binding properties, we synthesized and analyzed phenanthridinium chromophores **1–4** experimentally as well as theoretically, and compared them with **E**. The optical and electrochemical properties, as well as the DNA titration and binding experiments, reveal two chromophore pairs. The first pair, consisting of dyes **1** and **2** and lacking the amino substituents in positions 3 and 8, exhibits clearly altered optical and electrochemical properties than those of **E**. A significant fluorescence quenching of these compounds is observed in the presence of DNA. Their binding affinity to DNA is reduced by nearly one order of magnitude. The electronic effect of the phenyl group in position 6 on this type of phenanthridinium dye is rather small.

The optical and redox properties of the second set of chromophores, **3** and **4**, are similar to **E**. It is known that the presence of the two electron-donating amino groups in positions 3 and 8 of the phenanthridinium heterocycle has a significant electronic influence and supplies electron density to the endocyclic iminium core. However, it is important to note that, in contrast to compounds **1** and **2**, the electron-donating character of the phenyl ring in position 6 of chromophores **3** and **4** is additionally critical for the characteristic and unique fluorescence behavior of these dyes, especially in the presence of DNA. The binding, as well as fluorescence, is clearly related to the electron-donating character of this substituent. Accordingly, dye **4** shows both the strongest binding affinity and the strongest fluorescence enhancement. This is a remarkable result and is of potential interest for the future design of fluorescent probes for nucleic acids. Quantum chemical calculations reveal a general mechanism that is based on TICT-like states. A CT state can be reached by twisting the phenyl ring in position 6 towards 90° with respect to the phenanthridinium core. The properties of this TICT-like excited state are such that fluorescence quenching occurs. The energetic availability of the CT state depends on the electron-donating character of the phenyl group and changes upon binding to DNA. Moreover, the rigidity of DNA hinders the formation of CT. This mechanism repre-

sents an important addition to the previous proposal of protonation in the excited state and can help to optimize the performance of the fluorescence enhancement factor of future fluorescent probes for nucleic acids.

Acknowledgements

This work was generously financed by the Deutsche Forschungsgemeinschaft and by the Graduate College "Sensory Photoreceptors in Natural and Artificial Systems" (GRK640).

- [1] S. L. Lerman, *J. Mol. Biol.* **1961**, 3, 18–30.
- [2] a) V. K. Misra, B. Honig, *Proc. Natl. Acad. Sci. USA* **1995**, 92, 4691–4695; b) S. E. Patterson, J. M. Coxon, L. Stekowski, *Bioorg. Med. Chem.* **1997**, 5, 277–281; c) C. Medhi, J. B. O. Mitchell, S. L. Price, A. B. Tabor, *Biopolymers* **1999**, 52, 84–93; d) D. Reha, M. Kabeláč, F. Ryjáček, J. Šponer, J. E. Šponer, M. Elstner, S. Suhai, P. Hobza, *J. Am. Chem. Soc.* **2002**, 124, 3366–3376.
- [3] H. Ihmels, D. Otto, *Top. Curr. Chem.* **2005**, 258, 161–204.
- [4] a) G. Viola, F. Dall'Acqua, N. Gabellini, S. Moro, D. Vedaldi, H. Ihmels, *ChemBioChem* **2002**, 3, 550–558; b) G. Viola, M. Bressanini, N. Gabellini, D. Vedaldi, F. Dall'Acqua, H. Ihmels, *Photochem. Photobiol. Sci.* **2002**, 1, 882–889.
- [5] a) H. Ihmels, K. Faulhaber, K. Wissel, G. Viola, D. Vedaldi, *Org. Biomol. Chem.* **2003**, 1, 2999–3001; b) A. Granzhan, H. Ihmels, G. Viola, *J. Am. Chem. Soc.* **2007**, 129, 1254–1267.
- [6] a) A. R. Morgan, J. S. Lee, D. E. Pulleyblank, N. L. Murray, D. H. Evans, *Nucleic Acids Res.* **1979**, 7, 547–569; b) A. R. Morgan, D. Evans, J. S. Lee, D. E. Pulleyblank, *Nucleic Acids Res.* **1979**, 7, 571–594.
- [7] H. Nishiwaki, M. Miura, K. Imai, R. Ohno, K. Kawashima, *Cancer Res.* **1974**, 34, 2699–2703.
- [8] a) R. V. Guntaka, B. W. Mahy, J. M. Bishop, H. E. Varmus, *Nature* **1975**, 253, 507–511; b) N. W. Luedtke, Y. Tor, *Biopolymers* **2003**, 70, 103–119.
- [9] a) J. N. A. Tettey, G. G. Skellern, M. H. Grant, J. M. Midgley, *J. Pharm. Biomed. Anal.* **1999**, 21, 1–7; b) J. N. A. Tettey, G. G. Skellern, J. M. Midgley, M. H. Grant, A. R. Pitt, *Chem.-Biol. Interact.* **1999**, 123, 105–115.
- [10] a) M. J. Waring in *Antibiotics III Mechanism of Action of Antimicrobial and Antitumour Agents* (Eds.: J. W. Corcoran, F. E. Hahn), Springer, Heidelberg, **1975**, pp. 141–165; b) L. P. G. Wakelin, M. J. Waring, *J. Mol. Biol.* **1980**, 144, 183–214.
- [11] a) V. L. Singer, T. E. Lawlor, S. Yue, *Mutat. Res.* **1999**, 439, 37–47; b) M. Fukunaga, B. A. Cox, R. S. von Sprecken, L. W. Yielding, *Mutat. Res.* **1984**, 127, 31–37; c) T. Ohta, S. Tokishita, H. Yamagata, *Mutat. Res.* **2001**, 492, 91–97; d) S. Hoare, R. B. Kemp, M. A. Kaderbhai, *Biochem. Soc. Trans.* **1993**, 21, 504.
- [12] a) B. Gaugain, J. Barbet, R. Oberlin, B. P. Roques, J.-B. Le Pecq, *Biochemistry* **1978**, 17, 5071–5078; b) B. Gaugain, J. Barbet, N. Cappelletti, B. P. Roques, J.-B. Le Pecq, *Biochemistry* **1978**, 17, 5078–5088; c) M. M. Becker, P. B. Dervan, *J. Am. Chem. Soc.* **1979**, 101, 3664–3666; d) K. F. Kuhlmann, C. W. Mosher, *J. Med. Chem.* **1981**, 24, 1333–1337; e) I. G. Lopp, W. D. Wilson, D. W. Boykin, *J. Heterocycl. Chem.* **1982**, 19, 695–696.
- [13] a) L. Benimetskaya, N. V. Bulychev, A. L. Kozionov, A. A. Koshkin, A. V. Lebedev, S. Y. Novozhilov, M. I. Stockman, *Biopolymers* **1989**, 28, 1129–1147; b) G. Krishnamurthy, T. Polte, T. Rooney, M. E. Hogan, *Biochemistry* **1990**, 29, 981–988.
- [14] a) R. F. Pasternack, M. Caccam, B. Keogh, T. A. Stephenson, A. P. Williams, E. J. Gibbs, *J. Am. Chem. Soc.* **1991**, 113, 6835–6840; b) W. J. Jin, Y. S. Wei, C. S. Liu, G. L. Shen, R. Q. Yu, *Spectrochim. Acta, Part A* **1997**, 53, 2701–2707.
- [15] a) P. Fromherz, B. Rieger, *J. Am. Chem. Soc.* **1986**, 108, 5361–5362; b) S. J. Atherton, P. C. Beaumont, *J. Phys. Chem.* **1987**, 91, 3993–3997; c) D. A. Dunn, V. H. Lin, I. E. Kochevar, *Biochemistry* **1992**, 31, 11620–11625; d) A. M. Brun, A. Harriman, *J. Am. Chem. Soc.* **1992**, 114, 3656–3660; e) S. J. Atherton, P. C. Beaumont, *J. Phys. Chem.* **1995**, 99, 12025–12029; f) A. I. Kononov, E. B. Moroshkina, N. V. Tkachenko, H. Lemmetyinen, *J. Phys. Chem. B* **2001**, 105, 535–541; g) P. T. Henderson, E. Boone, G. B. Schuster, *Helv. Chim. Acta* **2002**, 85, 135–151.
- [16] a) S. O. Kelley, R. E. Holmlin, E. D. A. Stemp, J. K. Barton, *J. Am. Chem. Soc.* **1997**, 119, 9861–9870; b) D. B. Hall, S. O. Kelley, J. K. Barton, *Biochemistry* **1998**, 37, 15933–15940; c) S. O. Kelley, J. K. Barton, *Chem. Biol.* **1998**, 5, 413–425; d) C. Wan, T. Fiebig, S. O. Kelley, C. R. Treadway, J. K. Barton, A. H. Zewail, *Proc. Natl. Acad. Sci. USA* **1999**, 96, 6014–6019.
- [17] a) N. Amann, R. Huber, H.-A. Wagenknecht, *Angew. Chem.* **2004**, 116, 1881–1883; *Angew. Chem. Int. Ed.* **2004**, 43, 1845–1847; b) L. Valis, N. Amann, H.-A. Wagenknecht, *Org. Biomol. Chem.* **2005**, 3, 36–38; c) L. Valis, Q. Wang, M. Raychev, I. Buchvarov, H.-A. Wagenknecht, T. Fiebig, *Proc. Natl. Acad. Sci. USA* **2006**, 103, 10192–10195.
- [18] R. Huber, N. Amann, H.-A. Wagenknecht, *J. Org. Chem.* **2004**, 69, 744–751.
- [19] M. Bahr, L. Valis, H.-A. Wagenknecht, E. Weinhold, *Nucleosides Nucleotides Nucleic Acids* **2007**, 26, 1581–1584.
- [20] J. Olmsted III, D. R. Kearns, *Biochemistry* **1977**, 16, 3647–3654.
- [21] L. P. G. Wakelin, M. J. Waring, *Mol. Pharmacol.* **1974**, 9, 544–561.
- [22] M. Le Bret, O. Chalvet, *J. Mol. Struct.* **1977**, 37, 299–319.
- [23] C. Mehdi, J. B. Mitchell, S. L. Price, A. B. Tabor, *Biopolymers* **1999**, 52, 84–93.
- [24] a) D. Reha, M. Kabeláč, F. Ryjáček, J. Šponer, J. E. Šponer, M. Elstner, S. Suhai, P. Hobza, *J. Am. Chem. Soc.* **2002**, 124, 3366–3376; b) T. Kubař, M. Hanus, F. Ryjáček, P. Hobza, *Chem. Eur. J.* **2006**, 12, 280–290.
- [25] W. Leupin, J. Feigon, W. A. Denny, D. R. Kearns, *Biophys. Chem.* **1985**, 22, 299–305.
- [26] N. W. Luedtke, Q. Liu, Y. Tor, *Chem. Eur. J.* **2005**, 11, 495–508.
- [27] W. J. Firth III, C. L. Watkins, D. E. Graves, L. W. Yielding, *J. Heterocycl. Chem.* **1983**, 20, 759–765.
- [28] a) L. W. Yielding, W. J. Firth III, *Mutat. Res.* **1980**, 71, 161–168; b) M. Fukunaga, L. W. Yielding, W. J. Firth III, K. L. Yielding, *Mutat. Res.* **1980**, 78, 151–157; c) M. Fukunaga, L. W. Yielding, *Mutat. Res.* **1983**, 121, 89–94; d) M. Fukunaga, Y. Mizuguchi, L. W. Yielding, K. L. Yielding, *Mutat. Res.* **1984**, 127, 15–21; e) F. Leng, D. Graves, J. B. Chaires, *Biochim. Biophys. Acta, Gene Struct. Expression* **1998**, 1442, 71–81.
- [29] L. W. Yielding, K. L. Yielding, J. E. Donoghue, *Biopolymers* **1984**, 23, 83–110.
- [30] a) G. Morgan, L. P. Walls, *J. Chem. Soc.* **1938**, 389–397; b) L. P. Walls, *J. Chem. Soc.* **1945**, 294–300.
- [31] T. I. Watkins, *J. Chem. Soc.* **1952**, 3, 3059–3064.
- [32] S. S. Berg, *J. Chem. Soc.* **1963**, 14, 3635–3640.
- [33] J. Loccufier, E. Schacht, *Tetrahedron* **1989**, 45, 3385–3396.
- [34] a) N. P. Gritsan, A. A. Koshkin, A. Y. Denisov, Y. Y. Markushin, E. V. Cherepanova, A. L. Lebedev, *J. Photochem. Photobiol. B* **1997**, 37, 40–51; b) N. Amann, H.-A. Wagenknecht, *Tetrahedron Lett.* **2003**, 44, 1685–1690; c) S. Rangarajan, S. H. Friedman, *Bioorg. Med. Chem. Lett.* **2007**, 17, 2267–2273.
- [35] J. N. Demas, G. A. Crosby, *J. Phys. Chem.* **1971**, 75, 991–1024.
- [36] D. F. Eaton, *Pure Appl. Chem.* **1988**, 60, 1107–1114.
- [37] a) A. Weller, *Z. Phys. Chem. (Muenchen Ger.)* **1982**, 133, 93–98; b) K. Kumar, I. V. Kurnikov, D. N. Beratan, H. D. Waldeck, M. B. Zimmt, *J. Phys. Chem. A* **1998**, 102, 5529–5541.
- [38] G. Cosa, K.-S. Foscaneanu, J. R. N. McLean, J. P. McNamee, J. C. Scaiano, *Photochem. Photobiol.* **2001**, 73, 585–599.
- [39] a) M. J. Waring, *J. Mol. Biol.* **1965**, 13, 269–282; b) J.-B. Le-Pecq, C. Paleotti, *J. Mol. Biol.* **1967**, 27, 87–106; c) R. L. Letsinger, M. E. Schott, *J. Am. Chem. Soc.* **1981**, 103, 7394–7396.
- [40] J. D. McGhee, P. H. von Hippel, *J. Mol. Biol.* **1974**, 86, 469–489.

- [41] a) H. W. Zimmermann, *Angew. Chem.* **1986**, 98, 115–131; *Angew. Chem. Int. Ed. Engl.* **1986**, 25, 115–130; b) J. Pauluhn, H. W. Zimmermann, *Ber. Bunsen-Ges.* **1979**, 83, 76–82.
- [42] E. D. Horowitz, N. V. Hud, *J. Am. Chem. Soc.* **2006**, 128, 15380–15381.
- [43] S. O. Kelley, J. K. Barton, *Chem. Biol.* **1998**, 5, 413–425.
- [44] V. V. Pavlishchuk, A. W. Addison, *Inorg. Chim. Acta* **2000**, 298, 97–102.
- [45] M. Torimura, S. Kurata, K. Yamada, T. Yokomaku, Y. Kamagata, T. Kanagawa, R. Kurane, *Anal. Sci.* **2001**, 17, 155–160.
- [46] H.-A. Wagenknecht, *Nat. Prod. Rep.* **2006**, 23, 973–1006.
- [47] N. C. Garbett, N. B. Hammond, D. E. Graves, *Biophys. J.* **2004**, 87, 3974–3981.
- [48] a) I. Juranovic, Z. Meic, I. Piantanida, L.-M. Tumir, M. Zinic, *Chem. Commun.* **2002**, 1432–1433; b) L.-M. Tumir, I. Piantanida, P. Novak, M. Zinic, *J. Phys. Org. Chem.* **2002**, 15, 599–607; c) L.-M. Tumir, I. Piantanida, I. J. Cindric, T. Hrenar, Z. Meic, M. Zinic, *J. Phys. Org. Chem.* **2003**, 16, 891–899; d) L.-M. Tumir, I. Piantanida, I. Juranovic, Z. Meic, S. Tomic, M. Zinic, *Chem. Commun.* **2005**, 2561–2563.
- [49] T. Förster, G. Hoffmann, *Z. Phys. Chem. (Muenchen Ger.)* **1971**, 75, 63.
- [50] a) M. Vogel, W. Rettig, *Ber. Bunsen-Ges.* **1985**, 89, 962–968; b) M. Vogel, W. Rettig, *Ber. Bunsen-Ges.* **1987**, 91, 1241–1247.
- [51] W. Rettig, *Angew. Chem.* **1986**, 98, 969–986; *Angew. Chem. Int. Ed. Engl.* **1986**, 25, 971–988.
- [52] Z. R. Grabowski, K. Rotkiewicz, W. Rettig, *Chem. Rev.* **2003**, 103, 3899–4031.
- [53] P. Plaza, N. Dai Hung, M. M. Martin, Y. H. Meyer, M. Vogel, W. Rettig, *Chem. Phys.* **1992**, 168, 365–373.
- [54] C. J. F. Böttcher in *Theory of electric polarization*, Elsevier, Amsterdam, **1973**, p. 42.
- [55] H. Ephardt, P. Fromherz, *J. Phys. Chem.* **1993**, 97, 4540–4547.
- [56] V. Kharlanov, W. Rettig, *Chem. Phys.* **2007**, 332, 17–26.

Received: October 13, 2009
Published online: February 19, 2010